Electronic Supplementary Material (ESI) for Physical Chemistry Chemical Physics.

Supporting Information:

Mechanistic Studies of Pyridinium Electrochemistry: Alternative Chemical Pathways in the Presence of CO_2

Alex G. Peroff, Eric Weitz, and Richard Van Duyne

Northwestern University, Department of Chemistry, Evanston IL, 60208

Table of Contents

For all digital simulations $k_{s,h}$ = heterogeneous rate constant and α = transfer coefficient, K_{chem} = rate of forward chemical step.

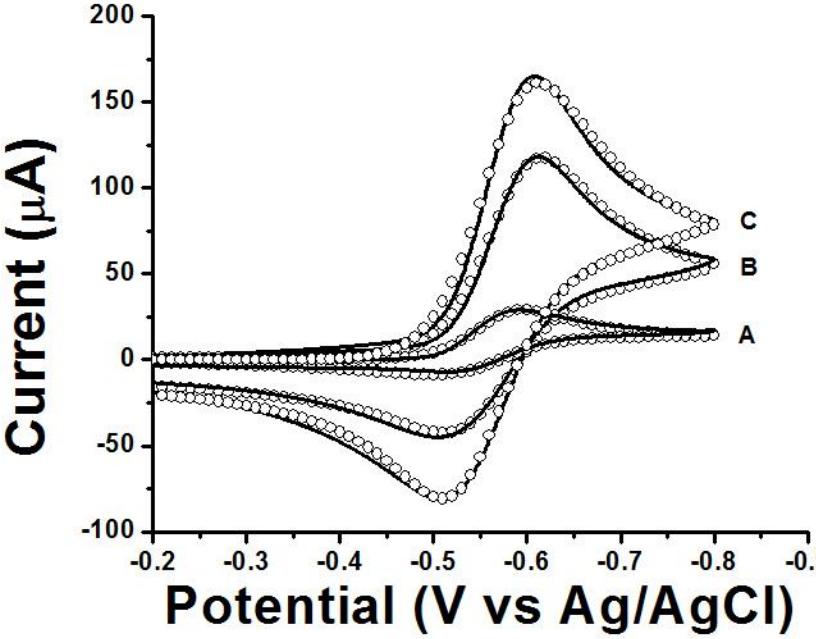

Figure S1: CV of 30 mM pyridine at pH 5.6 in 0.5 M KCl degassed in N_2 on Pt electrode at 5 (A), 100 (B), and 200 (C) mV/s (black), digital simulation (circles). A reversible electron transfer step followed by an irreversible chemical step was employed for simulations, Diffusion coefficient = 1.77×10^{-5} cm^2 s^{-1}, $k_{s,h}$ = 0.0083 cm s^{-1}, α = 0.59, K_{chem} = 0.11 s^{-1}. At faster scan rates the anodic wave increases relative to the cathodic wave.

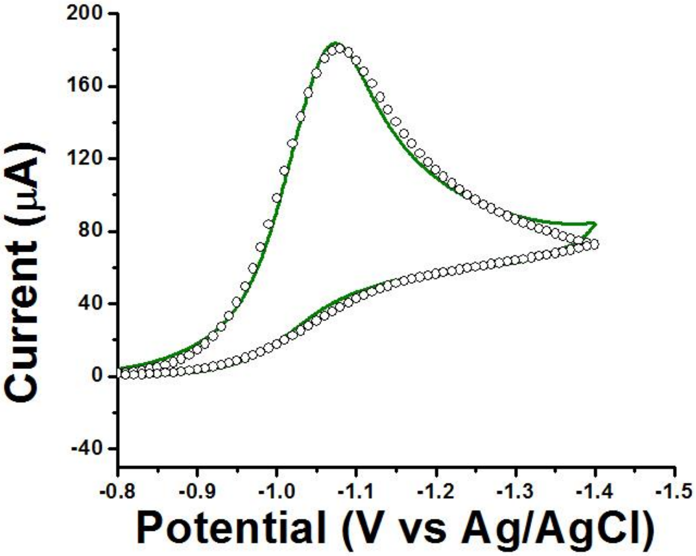

Figure S2: CV of 30 mM pyridine at pH 5.6 in 0.5 M KCl degassed in N_2 on Ag electrode at 100 mV/s (green), digital simulation (circles). A reversible electron transfer step followed by an irreversible chemical step was employed for simulations, Diffusion coefficient = 2.24 x 10^{-5} cm^2 s^{-1}, $k_{s,h}$ = 0.0091 cm s^{-1}, α = 0.57, K_{chem} > 10 s^{-1}.

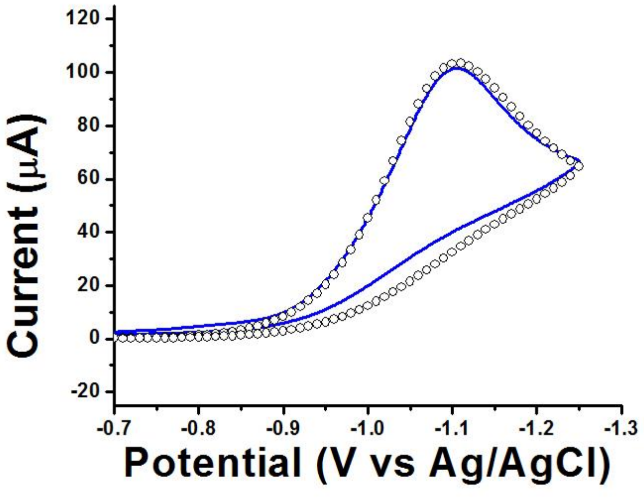

Figure S3: CV of 30 mM pyridine at pH 5.6 in 0.5 M KCl degassed in N_2 on Cu electrode at 100 mV/s (blue), digital simulation (circles). A reversible electron transfer step followed by an irreversible chemical step was employed for simulations, Diffusion coefficient = 8.89 x 10^{-6} cm^2 s^{-1}, $k_{s,h}$ = 0.006 cm s^{-1}, α = 0.49, K_{chem} > 10 s^{-1}.

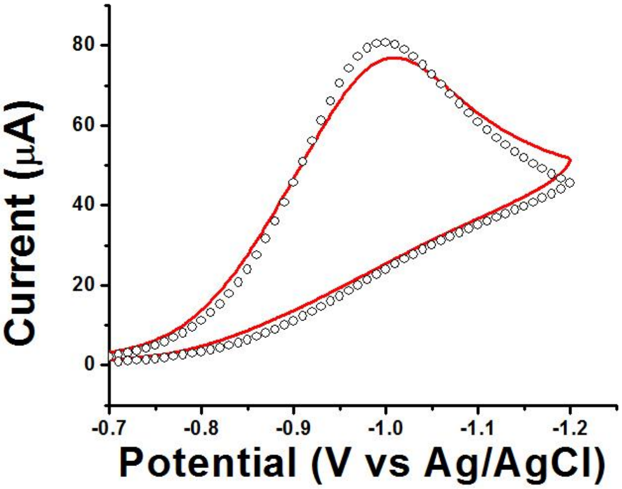

Figure S4: CV of 30 mM pyridine at pH 5.6 in 0.5 M KCl degassed in N_2 on Au electrode at 100 mV/s (red), digital simulation (circles). A reversible electron transfer step followed by an irreversible chemical step was employed for simulations, Diffusion coefficient = 1.71 x 10^{-5} cm^2 s^{-1}, $k_{s,h}$ = 0.002 cm s^{-1}, α = 0.49, K_{chem} > 10 s^{-1}.

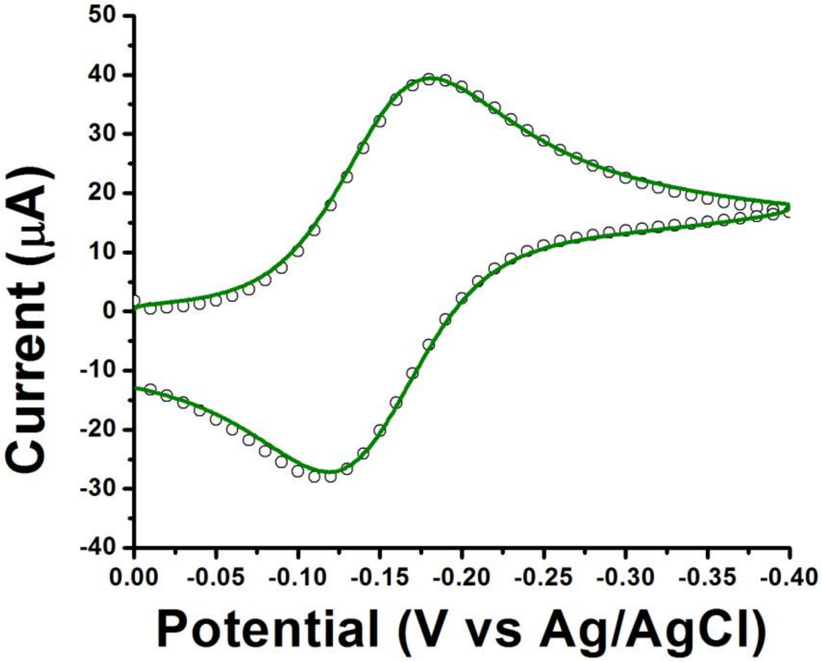

Figure S5: Cyclic voltammetry of 5 mM ruthenium hexamine on a Ag electrode 100 mV/s, 0.5 M KCl degassed in N_2 (green), digital simulation (circles) for an E mechanism with reversible 1e transfer, Diffusion coefficient = 8.94 x 10^{-6} cm^2 s^{-1}, $k_{s,h}$ = 0.39 cm s^{-1} , α = 0.5.

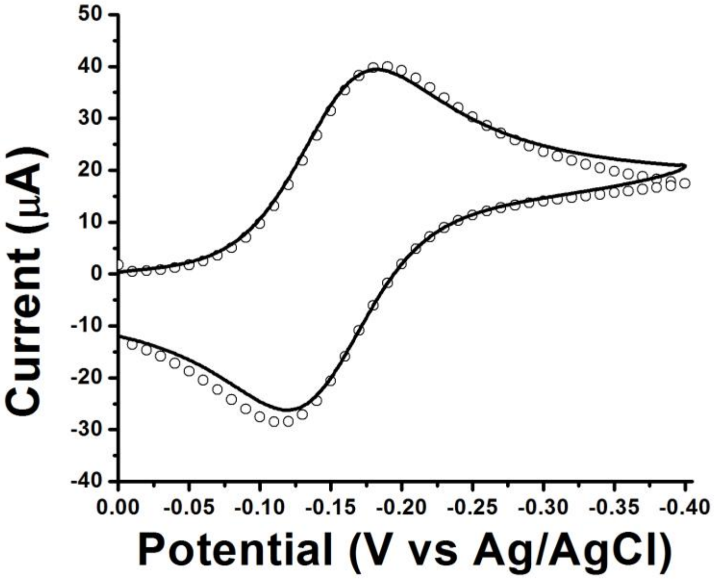

Figure S6: Cyclic voltammetry of 5 mM ruthenium hexamine on a Pt electrode 100 mV/s, 0.5 M KCl degassed in N_2 (black), digital simulation (circles) for an E mechanism with reversible 1e transfer, Diffusion coefficient = 8.67 x 10^{-6} cm^2 s^{-1}, $k_{s,h}$ = 0.35 cm s^{-1} , α = 0.49.

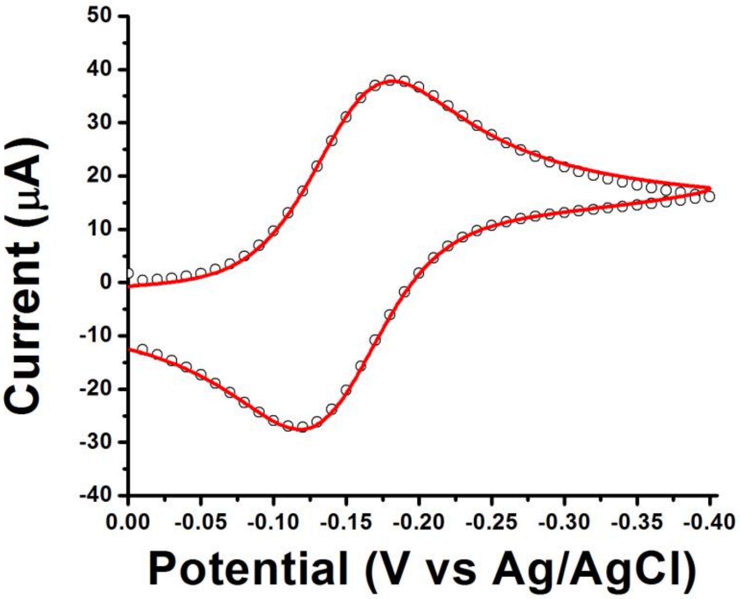

Figure S7: Cyclic voltammetry of 5 mM ruthenium hexamine on a Au electrode 100 mV/s, 0.5 M KCl degassed in N_2 (red), digital simulation (circles) for an E mechanism with reversible 1e transfer, Diffusion coefficient = 8.48 x 10^{-6} cm^2 s^{-1}, $k_{s,h}$ = 0.33 cm s^{-1} , α = 0.50.

Cyclic voltammetry of ruthenium hexamine could not be detected on copper electrodes because copper oxidizes near the reduction potential of ruthenium hexamine.

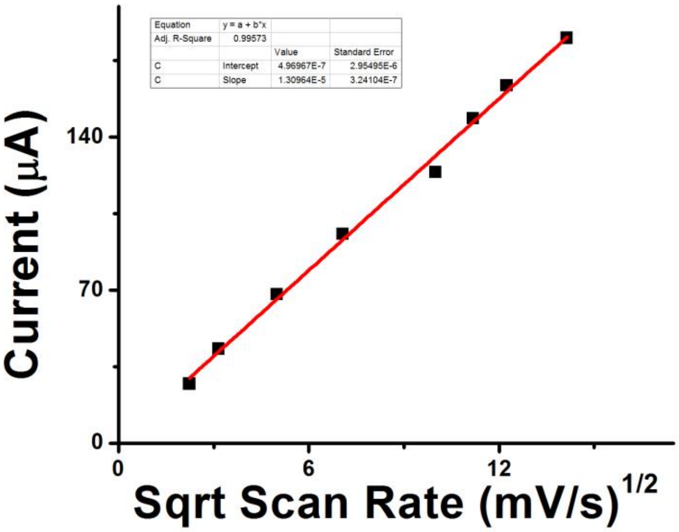

Equation	y = a + b*x		
Adj. R-Square	0.99573		
		Value	Standard Error
C	Intercept	4.96967E-7	2.95495E-6
C	Slope	1.30964E-5	3.24104E-7

Figure S8: Peak cathodic current vs the square root of the scan rate for pyridinium in the absence of CO_2 on Ag electrodes. Experimentally determined diffusion coefficient = 2.24 x 10^{-5} cm^2 s^{-1}

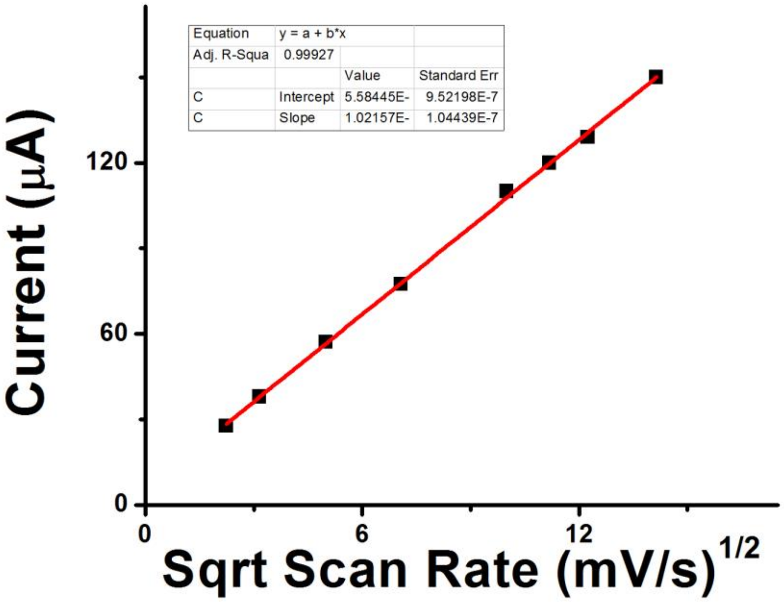

Equation	y = a + b*x		
Adj. R-Squa	0.99927		
		Value	Standard Err
C	Intercept	5.58445E-	9.52198E-7
C	Slope	1.02157E-	1.04439E-7

Figure S9 : Peak cathodic current vs the square root of the scan rate for pyridinium in the absence of CO_2 on Pt electrodes. Experimentally determined diffusion coefficient = 1.77 x 10^{-5} cm^2 s^{-1}

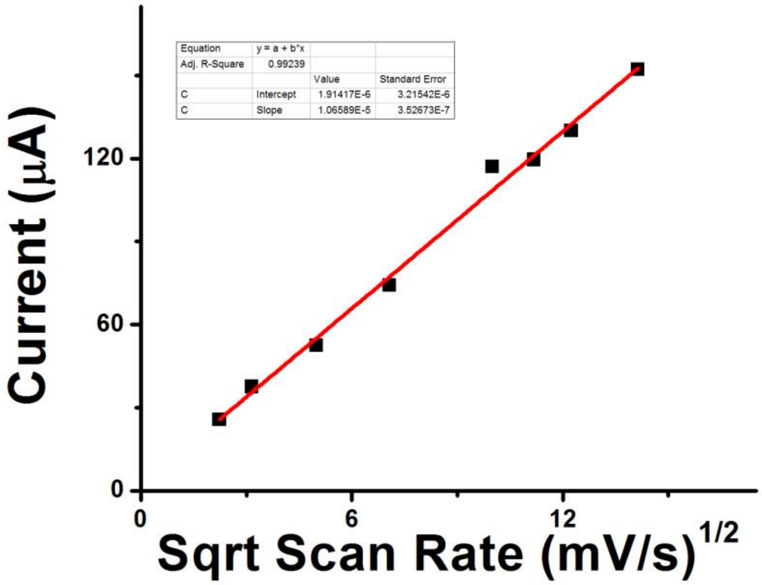

Equation	y = a + b*x		
Adj. R-Square	0.99239		
		Value	Standard Error
C	Intercept	1.91417E-6	3.21542E-6
C	Slope	1.06589E-5	3.52673E-7

Figure S10: Peak cathodic current vs the square root of the scan rate for pyridinium in the absence of CO_2 on Au electrodes. Experimentally determined diffusion coefficient = 1.71 x 10^{-5} cm^2 s^{-1}

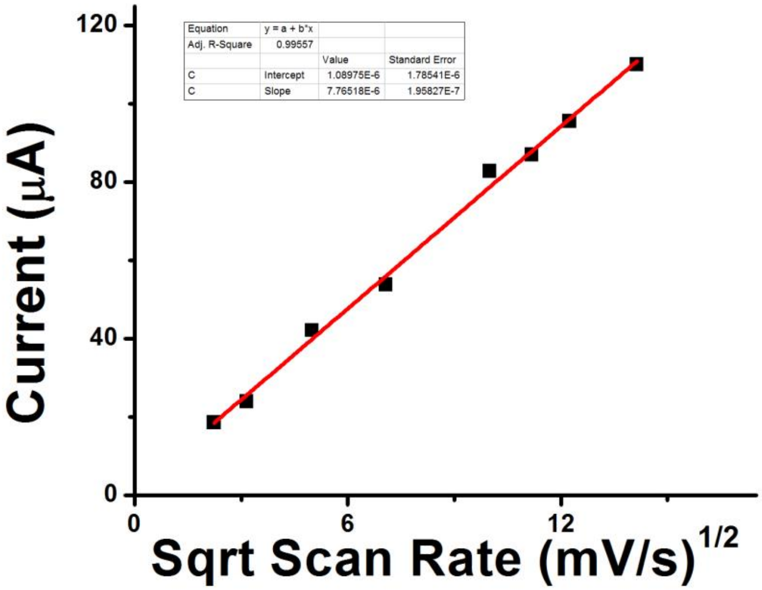

Equation	y = a + b*x		
Adj. R-Square	0.99557		
		Value	Standard Error
C	Intercept	1.08975E-6	1.78541E-6
C	Slope	7.76518E-6	1.95827E-7

Figure S11: Peak cathodic current vs the square root of the scan rate for pyridinium in the absence of CO_2 on Cu electrodes. Experimentally determined diffusion coefficient = 8.89 x 10^{-6} cm^2 s^{-1}

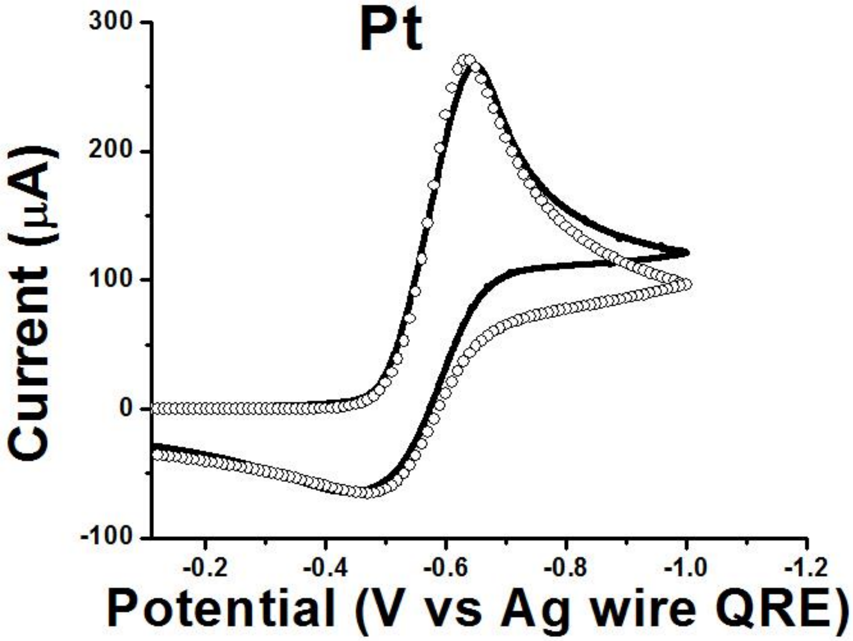

Figure S1: CV of Pt in acetonitrile with 30 mM pyridine, 30 mM perchloric acid, in 0.5 M $NaClO_4$ at 100 mV/s, degassed in N_2 (black), digital simulation (circles). A reversible electron transfer step followed by an irreversible chemical step was employed for simulations, Diffusion coefficient = 1.38 x 10^{-5} cm^2 s^{-1}, $k_{s,h}$ = 0.0077 cm s^{-1}, α = 0.50, K_{chem} = 0.3 s^{-1}.

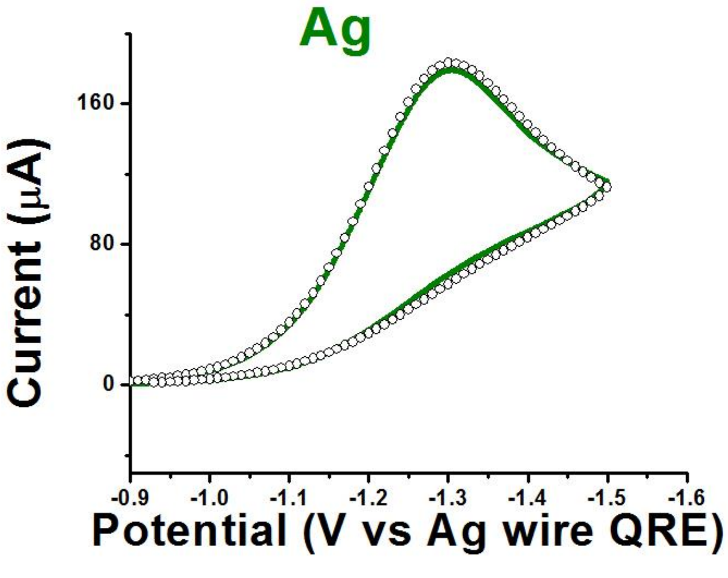

Figure S13: CV of Ag in acetonitrile with 30 mM pyridine, 30 mM perchloric acid, in 0.5 M $NaClO_4$ at 100 mV/s, degassed in N_2 (green), digital simulation (circles). A reversible electron transfer step followed by an irreversible chemical step was employed for simulations, Diffusion coefficient = 1.12 x 10^{-5} cm^2 s^{-1}, $k_{s,h}$ = 0.0073 cm s^{-1}, α = 0.47, K_{chem} > 10 s^{-1}.

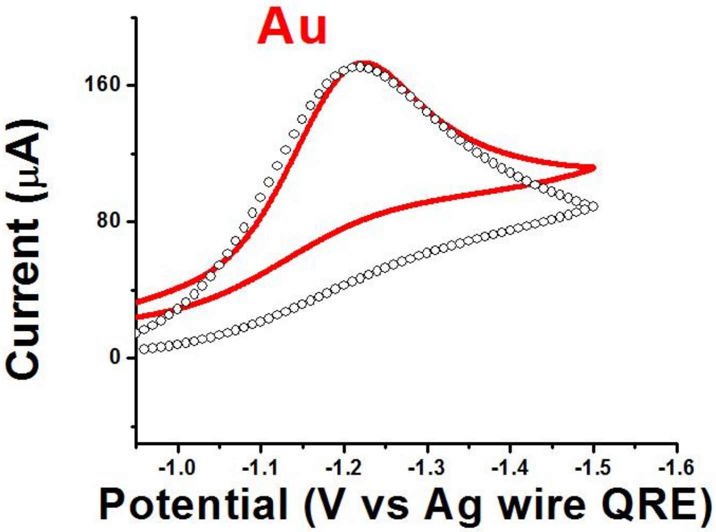

Figure S14: CV of Au in acetonitrile with 30 mM pyridine, 30 mM perchloric acid, in 0.5 M NaClO$_4$ at 100 mV/s, degassed in N$_2$ (red), digital simulation (circles). A reversible electron transfer step followed by an irreversible chemical step was employed for simulations, Diffusion coefficient = 1.11 x 10^{-5} cm^2 s^{-1}, k$_{s,h}$ = 0.0082 cm s^{-1}, α = 0.48, K$_{chem}$ > 10 s^{-1}.

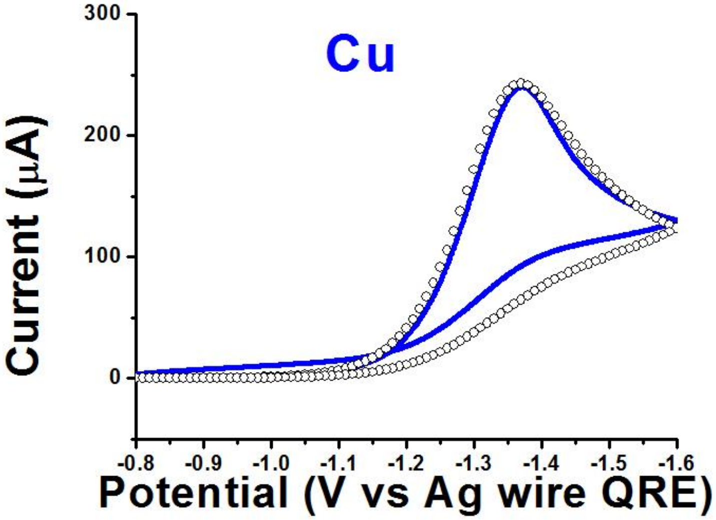

Figure S15: CV of Cu in acetonitrile with 30 mM pyridine, 30 mM perchloric acid, in 0.5 M NaClO$_4$ at 100 mV/s, degassed in N$_2$ (blue), digital simulation (circles). A reversible electron transfer step followed by an irreversible

chemical step was employed for simulations, Diffusion coefficient = 1.55 x 10^{-5} cm^2 s^{-1}, $k_{s,h}$ = 0.0071 cm s^{-1}, α = 0.48, K_{chem} > 10 s^{-1}.

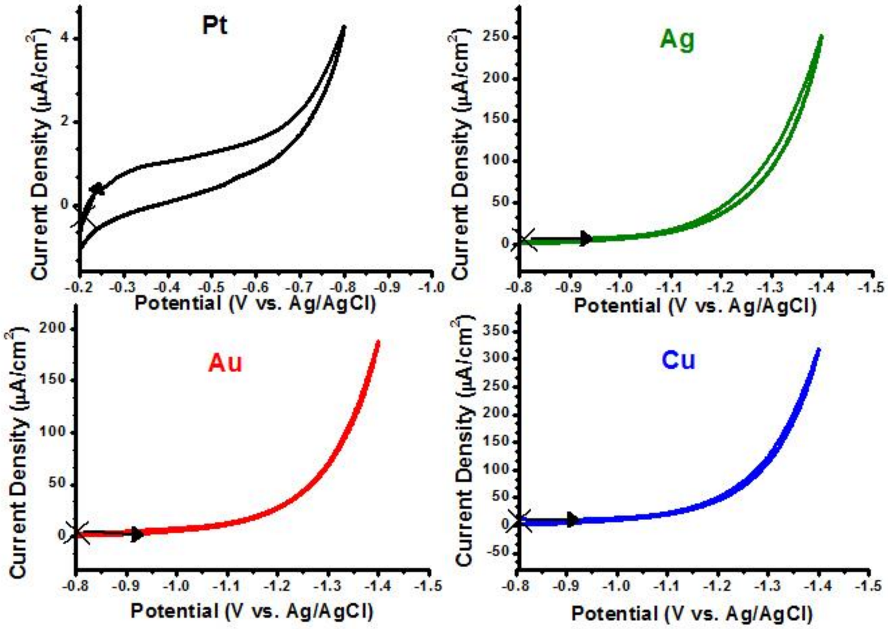

Figure S16 : CV's without pyridine, but with CO_2 buffered in K_2CO_3 to pH 5.6 at 5 mV/s. Electrodes are color coded Pt (black), Ag (green), Au (red), and Cu (blue).

S17 - SPECTROELECTROCHEMISTRY OF PYRIDINIUM ON COPPER

The method of preparation of film over nanosphere (FON) SERS active electrodes was adapted from previous literature procedures.[2,3] 540nm nm polystyrene spheres (Invitrogen) were diluted by a factor of 2 in milliQ water. The spheres were sonicated for ~ 15 minutes and vortexed for 1 minute. The spheres were then centrifuged at 10,000 rpm for 2.5 minutes. The supernatant was removed and fresh milliQ was added until the identical volume was achieved. This process was repeated 2 times to clean the sphere solution. A Kel-F plug with a copper lead was polished using a 1 μm alumina polish and sonicated in milliQ water for 1 minute. Kapton tape was used to mask off the sides of the electrode where metal contact was not desired. 400 nm of Cu was deposited on the plug using electron beam deposition at ~ 10^{-7} Torr. 10 μL of 400:1 methanol:tritonix solution was added on the 400 nm Cu electrode to wet the surface. 5 μL of the sphere solution was drop cast on top of the electrode; additional milliQ water was added to ensure that the solution covered the entire electrode surface. The electrode was rotated until the solution uniformly coated the electrode surface, and the solution was allowed to dry, leaving a hexagonally closed pack array of nanospheres on the surface. 200 nm Cu was deposited on the electrode using electron beam deposition at ~ 10^{-7} Torr.

The spectroelectrochemical cell consisted of flow cell made of Kel-F with a back side for the working electrode, and front side for a 18 mm glass cover slip. The cell has several side ports for the reference electrode, counter electrode, a mounting port, and several ports for injection of liquids and/or gases. The front of the cell consists of an 18 mm glass cover slip in between two rubber gaskets and screwed into the cell body with a metal front plate. The electrode is placed in-between two rubber gaskets and screwed into the cell body with a metal back plate. The counter electrode was coiled around the working electrode in order to maximize surface area in the cell without shorting the working electrode. A more thorough description of the cell is provided elsewhere.[4] The entire cell assembly is mounted to an optical post where laser light was focused onto the electrode surface, and back scattered Raman light was collected. The Raman scattered light was collected through a series of optical elements and focused into a 2500i Acton triple grating spectrometer (Princeton Instruments) and detected using a PIXIS CCD detector (Princeton Instruments). A 633 nm continuous wave HeNe (Voltex inc) laser at 7 mW power was used for all spectroelectrochemistry experiments. The spectrometer was calibrated using a cyclohexane spectrum. A CH instruments potentiostat was used to control the electrode potential during the SERS experiments.

Acknowledgements for SI

Dr. Alex Peroff was supported on the following grants for the following dates Chemical Sciences, Geosciences, and Biosciences Division, Office of Basic Energy Sciences, Office of Science, U.S. Department of Energy (Award No. DE-FG02-03-ER15457) January 2010 to May 2013; NSF CHE-1414466 June 2013 to Nov 2013; and AFOSR MURI FA9550-14-1-003 Dec 2013 to May 2014. Dr. Alex Peroff trained MURI students (Mike Mattei, Stephanie Zaleski, Xu Chen) and post-docs (Dmitry Kurouski) in electrochemistry. He also served as a consultant for Molecular Vista in the construction of a liquid cell used in the SECM-TERS instrument.

References for SI

(1) Conway, B. E.; Salomon, M. *Electrochimica Acta* **1964**, *9*, 1599.
(2) Dick, L. A.; McFarland, A. D.; Haynes, C. L.; Van Duyne, R. P. *The Journal of Physical Chemistry B* **2001**, *106*, 853.
(3) Paxton, W. F.; Kleinman, S. L.; Basuray, A. N.; Stoddart, J. F.; Van Duyne, R. P. *The Journal of Physical Chemistry Letters* **2011**, *2*, 1145.
(4) Miller, B. E., Northwestern University, 1989.